Journal of
Ceramic Science
and Technology

J. Ceram. Sci. Tech., **03** [02] 95-104 (2012)
DOI: 10.4416/JCST2012-00001
available online at: http://www.ceramic-science.com

Effects of Copper Oxide Content in AgCuO Braze Alloy on Microstructure and Mechanical Properties of Reactive-Air-Brazed $Ba_{0.5}Sr_{0.5}Co_{0.8}Fe_{0.2}O_{3-\delta}$ (BSCF)

A. Kaletsch*, A. Bezold, E.M. Pfaff, C. Broeckmann

Institute for Materials Applications in Mechanical Engineering, RWTH-Aachen University
received January 12, 2012; received in revised form January 24, 2012; accepted February 17, 2012

Abstract

For the joining of ceramic materials as well as ceramics and metals, reactive air brazing (RAB) is an important improvement compared to existing brazing technologies. In contrast to commonly used active brazing processes, no vacuum atmosphere is needed in RAB. This is a crucial factor for certain materials, such as some functional ceramics, which cannot be brazed in vacuum easily because they are thermodynamically unstable in atmospheres of low oxygen partial pressure. Sometimes for those materials, RAB is the only possibility to obtain a gas-tight sealing, which works safely up to high temperatures.

This paper presents current research findings concerning the influence of the copper oxide (CuO) content in AgCuO braze on the microstructure of the brazing zone and the mechanical properties of reactive-air-brazed ceramic/metal joints. The joining components are the perovskite-type ceramic $Ba_{0.5}Sr_{0.5}Co_{0.8}Fe_{0.2}O_{3-\delta}$ (BSCF) and the heat-resistant austenitic steel AISI 314. As braze materials, mixtures of silver with CuO contents between 1 mol% and 16 mol% were used.

The present study shows that a higher CuO content in the braze results in better wettability. However, a change in the microstructure of the ceramic can be observed, which becomes more pronounced with increased CuO concentration. This change in microstructure is characterized by higher and irregularly distributed porosity and increased grain sizes with copper cobalt oxide phases at the grain boundaries. Mechanical tests show that this reaction area leads to lower mechanical strength of the bonded specimens.

Keywords: RAB, reactive air brazing, perovskite, BSCF, CuO

I. Introduction

Ceramic components are becoming more and more important for many technical applications. Normally, ceramic components require joining to an adjacent metal structure. Joining ceramic to metal is a difficult task because of the insufficient wettability of metallic brazes on ceramics owing to high interfacial tensions and the handling of thermal stresses caused by different thermal expansion coefficients. Furthermore, ceramic materials are often integrated into high-temperature applications because of their high-temperature stability so that the seal usually needs to be heat-resistant. The most common joining technology applied to meet these requirements is active brazing. But active brazing needs a vacuum atmosphere and some functional ceramics, for example cathode materials like those used for Solid Oxygen Fuel Cells (SOFC), are not stable in atmospheres with very low oxygen partial pressures. Moreover, the perovskite-type $Ba_{0.5}Sr_{0.5}Co_{0.8}Fe_{0.2}O_{3-\delta}$ (BSCF), which is a promising high-temperature membrane material for oxygen separation from air, exhibits decomposition in a vacuum atmosphere [1]. BSCF membranes could be integrated in applications where pure oxygen is needed for any process, for example for oxygen supply in emission-free oxyfuel power plants [2]. The service temperature for BSCF membranes is between 800 °C and 900 °C. Here, the joints have to withstand the functional demands of the membranes while they are exposed to high mechanical loading at the same time.

As mentioned earlier, one typical problem of metal/ceramic bonds is the difference in the thermal expansion of the joining partners, leading to high thermal stresses during cooling from brazing temperature and at temperature cycles under service conditions. In the case of BSCF and the austenitic steel AISI 314 (DIN X15CrNiSi25 – 21, Werk.-Nr. 1.4841), the coefficients of thermal expansion (CTE) are almost equal. Both materials show high a CTE of $15*10^{-6}\ K^{-1}$ at room temperature and about $19*10^{-6}\ K^{-1}$ at 850 °C [3]. In this particular application, glass solders could be considered an alternative, but they are not applicable to join this material combination because their CTE is usually lower than $10*10^{-6}\ K^{-1}$. Wang *et al.* [4] and Shao *et al.* [5] used glass ceramic sealants to join BSCF in an oxygen permeation testing device. After measuring and cooling to room temperature, the thermal expansion mismatch damaged the sealant and membrane. With regard to the use of

* Corresponding author: A.Kaletsch@IWM.RWTH-Aachen.de

metal brazes, it is necessary to take into account that Oxygen Transport Membranes (OTM) work in an oxidizing atmosphere. Consequently, only noble metals can be used as braze material.

A brazing technology that might overcome the shortcomings of the technologies presented so far is reactive air brazing (RAB), for which Scott Weil applied for patent in the year 2002 [6]. Kim *et al.* [7] and Weil *et al.* [8,9] introduced this technology working with a silver-copper oxide (AgCuO) braze, which can be brazed in air atmosphere. The origin of this technology is "direct copper bonding" [10].

The principle of RAB is to braze in air with a braze alloy containing a noble metal as the base component and a metal that forms a metal oxide as the second component. In most cases silver is used as the noble metal and copper as the oxide builder. Hardy *et al.* [11] and Weil *et al.* [12] investigated the influence of the CuO content on the wetting behavior and mechanical properties of $La_{0.6}Sr_{0.4}Co_{0.2}Fe_{0.8}O_{3-\delta}$ (LSCF 6428) - joints. LSCF 6428 is a material that is chemically and crystallographically comparable to the investigated BSCF perovskite-type ceramic in this study and it is also used for OTM components. They demonstrated that "brazes containing 1.4 to 16 mol% CuO achieve the appropriate balance between braze composition, precipitate size, and morphology" [11]. In this range of CuO content no significant influence on the microstructure of the perovskite was observed. The three-point-bending strength of the joints amounted to more than "60 % of the intrinsic strength of monolithic LSCF-6428 substrates" [11]. For CuO contents higher than 34 mol%, the bending strength of the joints decreases. Weil *et al.* [13] investigated the influence of a low content of TiO_2 in the AgCuO braze on the wettability on LSCF 6428 and found out that the addition of TiO_2 leads to better wettability. But at the same time, a reaction zone in the LSCF 6428 appeared, "where evidence of grain boundary melting was observed" [13].

Bobzin *et al.* [14] investigated the thermo chemistry of brazing BSCF on AISI 314 with AgCuO braze and found strong reactions between the braze and BSCF, which leads to "thick reaction zones" in the ceramic.

The scope of this work is to estimate the reactions between the braze and BSCF in dependence on the CuO content in the braze alloy. Furthermore. it is necessary to consider if those reactions have any effect on the strength of BSCF/AgCuO/steel bonds.

II. Experimental

(1) Materials

BSCF 5582 powder (Treibacher, Austria) with an average grain size of 2.7 μm was granulated by means of spray granulation to granules with an average size of 125 μm. The chemical composition of the BSCF ceramic, measured with electron microprobe analysis (average of 8 points), is shown in Table 1.

Table 1: Chemical composition of the ceramic BSCF 5582 in mol%.

Ba	Sr	Co	Fe	O
11.01 ± 0.16	11.29 ± 0.08	17.07 ± 0.18	4.26 ± 0.05	56.37 ± 0.18

For the wetting tests, the BSCF granulate was uniaxially pressed with a pressure of 180 MPa to pellets with a diameter of 20 mm and a height of 4 mm. After pressing, the pellets were sintered in air at 1100 °C for 5 h. The braze alloy for the wetting test consists of silver powder (99.99 Alpha Caesar) doped with copper powder with varying concentrations from 1 mol% to 16 mol%. The Ag-Cu powder mix was uniaxially pressed in pellets with a diameter of 6 mm and a height of 1 mm. The description of the braze alloys with different concentrations is shown in Table 2.

Table 2: Chemical composition of the braze in mol% (measuring accuracy is 0.2 mol%).

	CuO	Ag
Ag1CuO	1	99
Ag1.4CuO	1.4	98.6
Ag2CuO	2	98
Ag3CuO	3	97
Ag4CuO	4	96
Ag6CuO	6	94
Ag8CuO	8	92
Ag10CuO	10	90
Ag12CuO	12	88
Ag14CuO	14	86
Ag16CuO	16	84

For the bond specimens a heat-resistant austenitic steel of grade AISI 314 was used. The chemical composition of the steel, measured by means of arc emission spectroscopy (average of 5 points) is shown in Table 3.

(2) Specimen geometry

For the wetting tests, the smaller braze pellets were placed on the sintered BSCF pellets (d = 17 mm). This assembly was placed in a furnace (Thermo-Star, Denta-Star M2). For tensile specimens, shown in Fig. 1, the BSCF was compressed by means of cold isostatic pressing at a pressure of 180 MPa to tubes. After sintering at 1100 °C in air for 5 h, the tubes have a length of 500 mm, a diameter of 15.5 mm and a wall thickness measuring 0.85 mm. The sintered tubes were cut with a diamond cutting wheel into pieces with a length of 10 mm and the cutting edges were manually ground with 1200-grit SiC paper. The BSCF pieces were brazed between two sleeves of the AISI 314 steel.

Table 3: Chemical composition of the steel AISI 314 (DIN X15CrNiSi25 – 21) in mass%.

C	Si	Mn	Cr	Ni	Fe	P	S
0.07 ± 0.004	2.02 ± 0.016	1.84 ± 0.012	24.74 ± 0.110	19.34 ± 0.068	51.00 ± 0.071	0.034 ± 0.001	0.001 ± 0.000

The chosen geometry allows subsequent mechanical testing of the specimens. The metal sleeves have internal screw threads, to assemble the bonded specimens with thread adapters into a testing machine for tensile tests.

Between the steel and BSCF component, two pieces of brazing foil were positioned. This foil was cut into rings with an outer diameter of 16 mm and an inner diameter of 13 mm. The brazing foil consists of a pure silver foil with a thickness of 70 μm and a galvanized copper layer on both sides, whereby a copper concentration of 3 mol% and alternatively 16 mol% was chosen. Fig. 2 shows by way of example a cross-section of the Ag16Cu brazing foil, with the pure silver substrate inside and the galvanized copper layers outside.

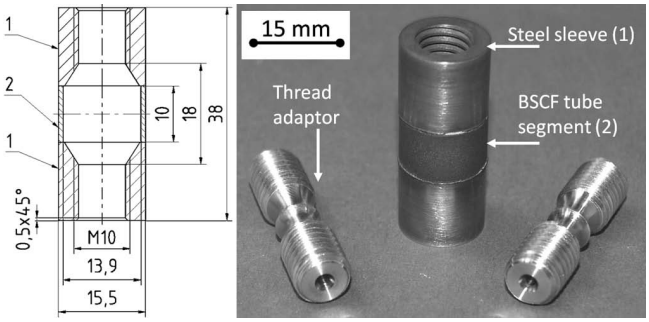

Fig. 1: Assembly of a brazed tensile specimen with thread adaptors.

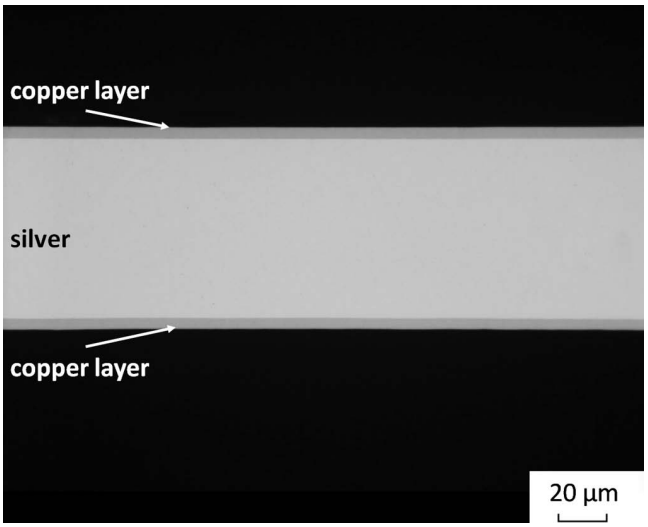

Fig. 2: Cross-section of a piece of brazing foil.

This type of geometry was chosen to reproduce the real design of tubular oxygen transport membranes. For the final application, 500 mm long BSCF tubes with a diameter of 15.5 mm have to be joined to metal sleeves, to integrate them into a pilot module for oxygen separation [15, 16]. Up to now the tubes have been joined with epoxy glues. But when glues are used, the joint patch has to be cooled down to temperatures below 200 °C and that means a reduction in the efficiency of the entire process. A non-cooled joint patch would have to fulfill certain requirements: it has to be gas-tight at high temperatures over a long period to guarantee a high purity of the supplied oxygen and furthermore it has to withstand stresses caused by the working pressure and thermal cycling under services conditions.

(3) Processing

The brazing temperature is 955 °C with a dwell time of 0.2 h. The brazing profile is shown in Fig. 3. A 1-h dwell time at 600 °C during cooling was introduced in order to reduce the internal stresses in the ceramic/steel joints, which had been proven in the authors' own finite element calculations. Major mechanisms for this are the homogenization of the temperature field and stress relaxation in the metal components of the joint.

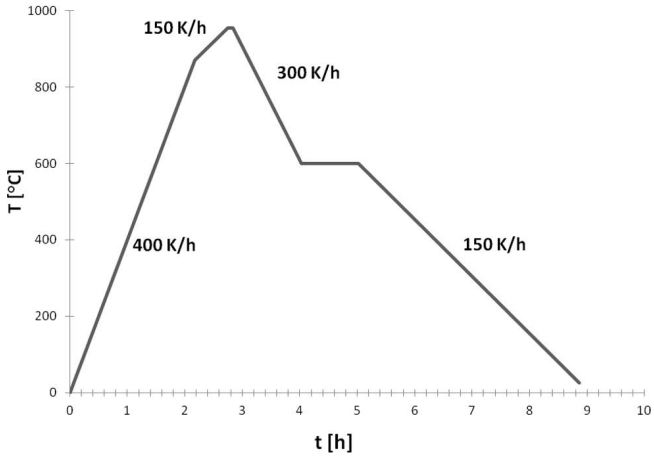

Fig. 3: Brazing profile.

(4) Finite element simulation

Finite element analysis (FEA) was used to predict the residual stress state in the joint during cooling from brazing temperature to room temperature. Residual stresses arise owing to the difference in the coefficient of thermal expansion (CTE) of the AISI 314 and the BSCF. The metal component wants to contract more upon cooling but is constrained at the interface. The brazing profile used for simulation is shown in Fig. 3 and the joint geometry in Fig. 13 (a) respectively. The joints were assumed to be perfectly bonded at the interface, the presence of voids in braze was ignored. The impact of metallurgical reactions of the joint materials during brazing was not taken into account. Further, it is assumed that the materials are stress-free at brazing temperature.

Axisymmetric, 4-node reduced integration elements were used in Abaqus 6.10 for constructing the model. On account of the symmetry, only a half model of the joint was analyzed and the nodes lying on the plane of symmetry were constrained in axial direction. The BSCF ceramic was considered to be linear-elastic. For AISI 314 steel, elasto-plastic behavior and isotropic hardening were

used. It is assumed that the material behavior of both braze options Ag16CuO and Ag3CuO is described accurately enough by a visco-plastic constitutive equation for pure silver. The uniaxial creep strain rate $\dot{c}_{cr}$ is given by Eq. (1).

$$\dot{c}_{cr} = A \cdot \sigma_{eq}^{n} \quad (1)$$

Eq. (1) is known as the Norton-Bailey law, where σ_{eq} is the equivalent deviatoric stress, *A* and *n* are constants depending on temperature. The physical properties of the joint materials can be found in Table 4.

III. Results and Discussion

(1) Microstructural characterization

After brazing, a cross-section of the interfaces was polished. The cross-section of the wetting specimens was used to determine the contact angle and to analyze the reactions between the joining partners and the braze alloy.

The cross-section was analyzed with the light microscope (LM) Axiophot from Zeiss and a scanning electron microscope (SEM) of the type JEOL JSM 6400. The contact angle was measured geometrically from the LM images.

It can be observed in Fig. 4 that with a higher CuO concentration the contact angle of the braze on a BSCF substrate decreases from 55° in the case of Ag1.4CuO to 34° in the case of Ag16CuO, and at the same time formation of affected zones indicated by a change of microstructure in the ceramic increases.

The dependence of the CuO content in the braze alloy on the wettability of BSCF is shown by Fig. 5. In general it can be expected that a low contact angle is preferable for brazed joints because that indicates better brazeability. Kim *et al.* [7,19] showed that the four-point-bending strength of Al_2O_3/AgCuO/Al_2O_3 and YSZ/AgCuO/YSZ joints with CuO concentrations between 1 mol% and 8 mol% rises with increasing wettability. But the wetting angle is not the only quantity influencing the bond strength. In the case of BSCF, a layer with microstructural changes is visible in the ceramic below the braze droplet. The higher the CuO content, the more serious is the change in microstructure.

In the following, the area of the changed microstructure is termed the affected zone. This affected zone was characterized with image analyze software (analySIS) that works with detected LM images. Thereby the thickness of the layer below the braze drop is measured at six different positions per specimen.

Fig. 6 shows the measured dependence of the CuO concentration on the thickness of the affected zone in the BSCF. Average thickness of the affected zone in the ceramic after brazing with Ag16CuO amounts to 520 μm (Fig. 7) whereas the affected zone with the Ag3CuO braze is measured with 180 μm.

	Temp. [°C]	E modules [GPa]	Poisson ratio ν [-]	Yield strength σ_Y [MPa]	CTE [10^{-6}1/K]	A [1/MPa]	n [-]
BSCF	20	63.2	0.25	n/a	14.7	n/a	n/a
	400	51.3			13.3		
	600	53.3			15.7		
	800	48.6			18.2		
Silver	20	76.0	0.37	63.0	19.4	-	-
	400	64.0	0.37	49.0	21.0	5.90E-19	8.30E+00
	600	55.0	0.38	22.0	21.3	1.20E-16	8.30E+00
	800	45.0	0.39	17.0	21.7	1.30E-08	2.55E+00
AISI314	20	196	0.30	292	15.7	n/a	n/a
	400	196	0.32	189	17.2		
	600	154	0.33	161	18.0		
	800	137	0.30	137	18.6		

Table 4: Physical properties of joint materials [17,18]

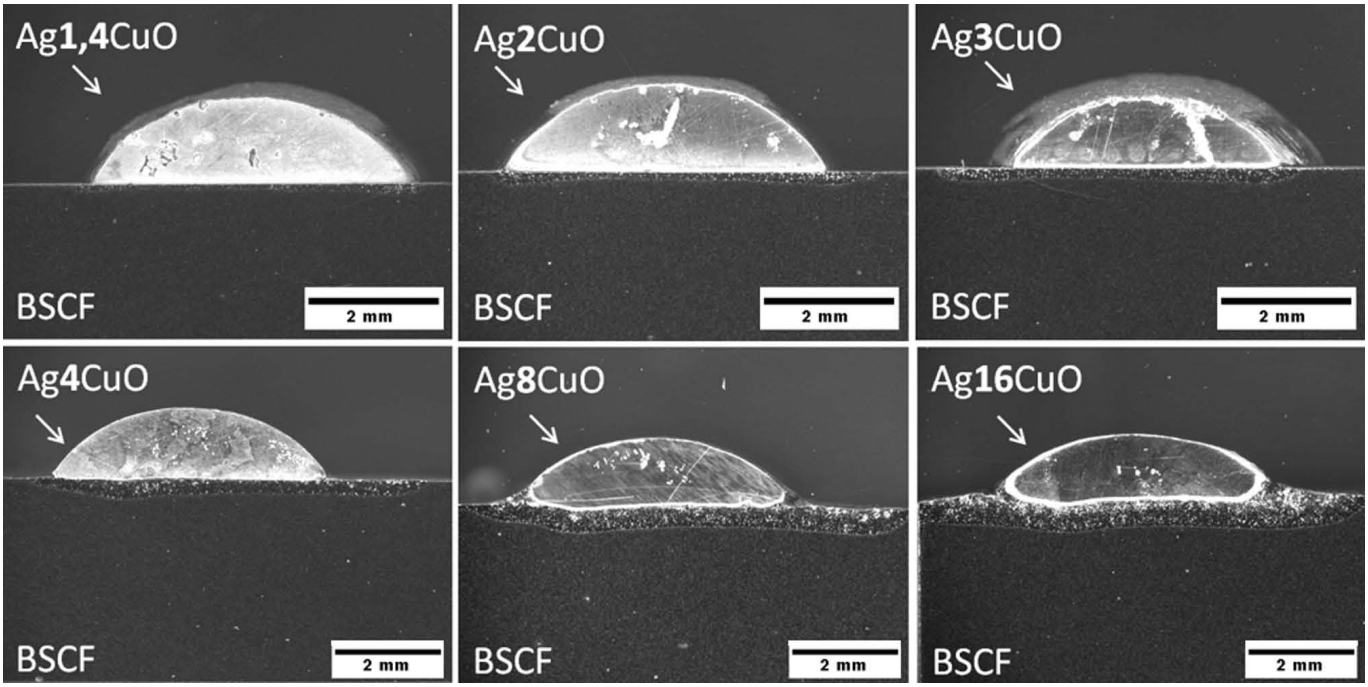

Fig. 4: Cross-section of wetting specimens (Ag*x*CuO on BSCF) with different CuO concentrations in the braze (T_b = 955 °C, t_d = 0.2 h).

A reason for the change in microstructure can be found in the CuO diffusion into the ceramic. Fig. 8 shows an SEM image of the area of the changed microstructure. New phases are visible in the BSCF. Energy-dispersive X-ray spectroscopy (EDX) analyses detect that these phases only consist of copper, cobalt and oxygen. Driessens *et al.* [20] and Zabdyr *et al.* [21] investigated the phase equilibria in the cobalt oxide (CoO)/CuO system and reported that CoO exhibits high solubility in CuO at temperatures above 900 °C. At 900 °C CuO is able to dissolve about 5 % CoO [20, 21].

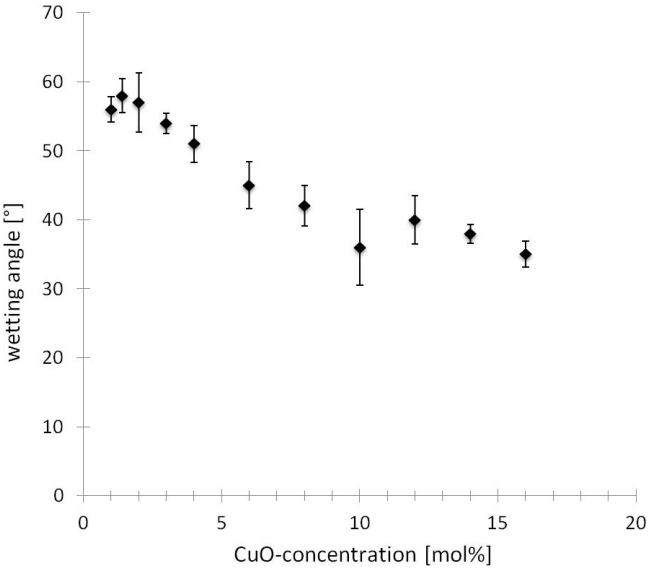

Fig. 5: Dependence of the CuO concentration in the braze on the wetting angle (T_b = 955 °C, t_d = 0.2 h).

In addition, bigger pores are visible. Whereas the unmodified BSCF structure shows fine and uniform porosity, the pores in the affected zone are larger and irregularly distributed. Caused by CuO diffusion along the grain boundaries and dissolving of CoO into the CuO within the affected zone, an increased sintering activity can be assumed.

That leads to local re-sintering of the material during the brazing process and an accumulation of pores. The re-sintering process is accompanied by grain growth, as illustrated in Fig. 9. In the upper part of the micrograph big grains and larger pores can be found in the affected layer whereas the lower part of the micrograph clearly shows the unaffected BSCF structure.

Also a higher porosity in the affected zone can be observed. Image analysis using LM reveals that the porosity increases drastically from the unaffected bulk material to the seam of the joint. Fig. 10 shows the distribution of porosity in the affected layer of a specimen brazed with Ag16CuO braze. This increased porosity could influence the mechanical properties of brazed specimens, as described in the next section.

Additionally the porosity leads to infiltration of the silver into the ceramic, as shown in Fig. 11. This effect is supported by the fact that compressive axial stress is used during the brazing process to reach acceptable bond strength.

The influence of the infiltrated silver is not yet clear; it has to be investigated in future with thermal cycling tests. It can be expected that in the case of temperature gradients the infiltrated silver causes tensile stresses in the ceramic owing to the CTE mismatch of silver and BSCF.

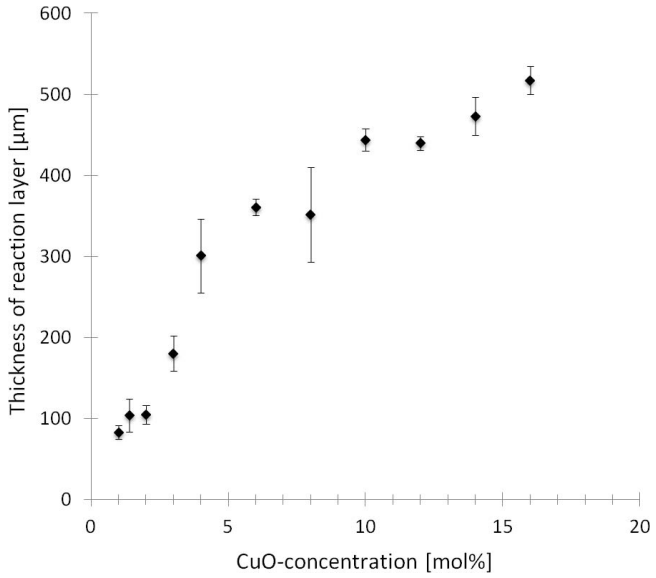

Fig. 6: Dependence of the CuO concentration in the braze on the thickness of the affected zone in the BSCF ceramic (T_b = 955 °C, t_d = 0.2 h).

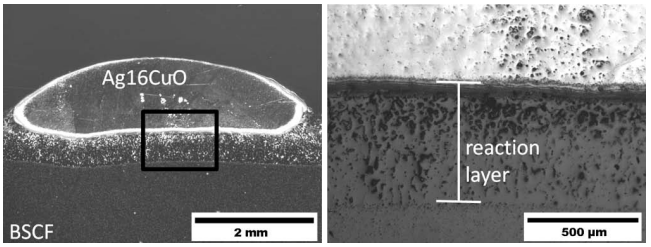

Fig. 7: Area of changed microstructure in the BSCF ceramic.

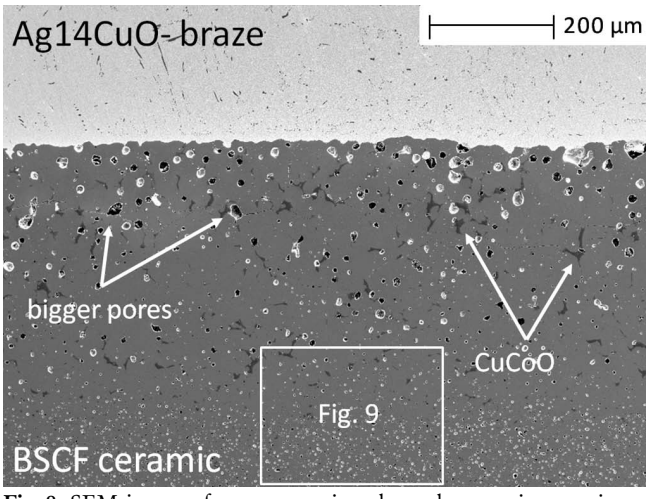

Fig. 8: SEM image of a cross-section through a wetting specimen (Ag14CuO on BSCF, T_b = 955 °C, t_d = 0.2 h).

(2) Mechanical characterization

To estimate the joint strength, several methods can be used which differ mainly in the loading system. Here it was decided to measure the strength with tensile tests, which is of course not commonly done in the characterization of ceramics. Three- or four-point bending tests are usually preferred, in order to realize a well-defined and reproducible load case. The problem in tensile testing is that very small amounts of superimposed bending stresses immediately influence the fracture force significantly. Nevertheless, with the particular application for the joints in mind, it was decided to test tubular joints under tensile load in order to analyze a comparable stress state and effective volume respectively. Therefore, special attention was paid to avoiding superimposed bending.

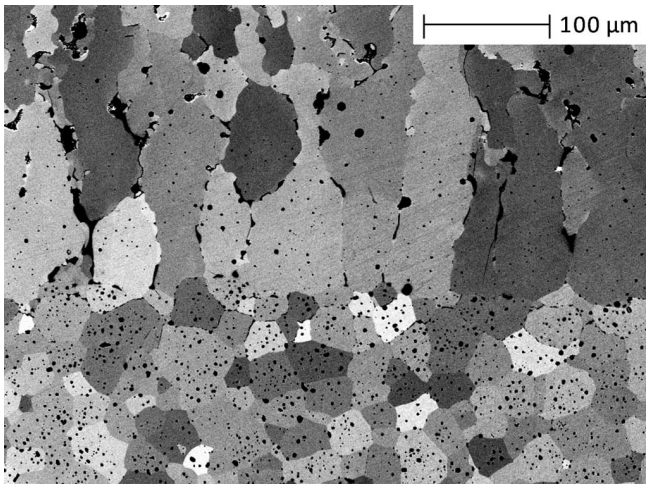

Fig. 9: SEM image of the microstructure in the BSCF in the brazing influence zone (Ag14CuO on BSCF, section from Fig. 8).

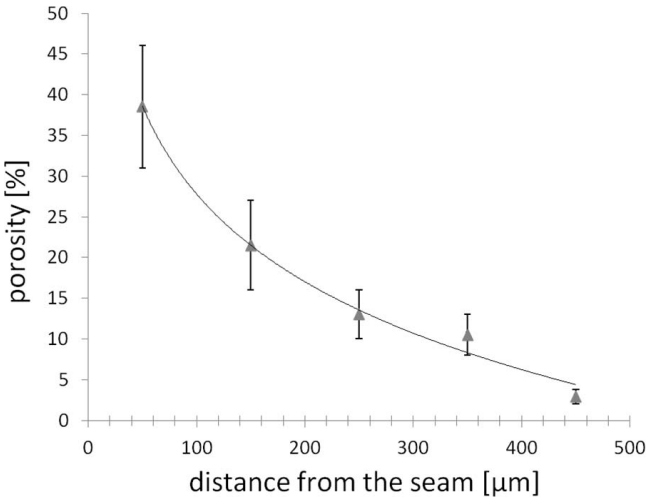

Fig. 10: Porosity in BSCF with Ag16CuO braze measured with image analysis.

A total of 24 tensile specimens brazed with the Ag3CuO braze and 16 tensile specimens brazed with the Ag16CuO braze (five specimens failed during assembly) were tested at room temperature in a Zwick ZMART-PRO test machine with an elongation rate of 0.02 mm/min. Primary failure mode for both braze options observed in the tensile-tested specimens was failure in the ceramic. A two-parameter Weibull distribution function in accordance with Eq. (2) was used to describe the strength distribution of the metal-to-ceramic braze joints.

$$F(\sigma_i) = 1 - \exp\left[-\frac{V_{eff}}{V_0}\left(\frac{\sigma_i}{\sigma_{0V}}\right)^m\right] \quad (2)$$

with

$$\sigma_{0V} = \sigma_0 \left(\frac{V_{eff}}{V_0}\right)^{\frac{1}{m}} \quad (3)$$

In Eqs. (2) and (3) V_0 is the unit volume, σ_i the single strength and F_i the corresponding failure probability.

V_{eff} is the effective volume, which is identical to the geometrical volume of the ceramic component in the tensile test. The strength distribution is then characterized with the Weibull modulus m and the characteristic strength σ_0, which depends on the material, size of the component and stress distribution in the joint, whereas σ_{0V} is independent of the volume and only depends on the material. Results of the measured tensile strength are shown in form of a Weibull plot in Fig. 12.

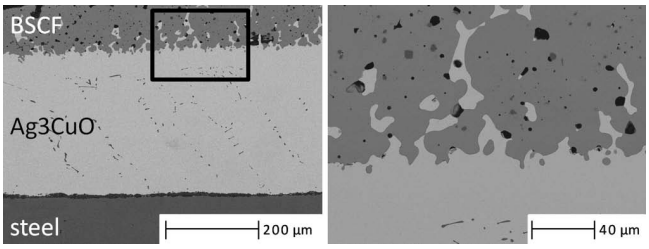

Fig. 11: SEM image of the interface of a brazed specimen (BSCF/AISI 314 with Ag3CuO-braze, T_b = 955 °C, t_d = 0.2).

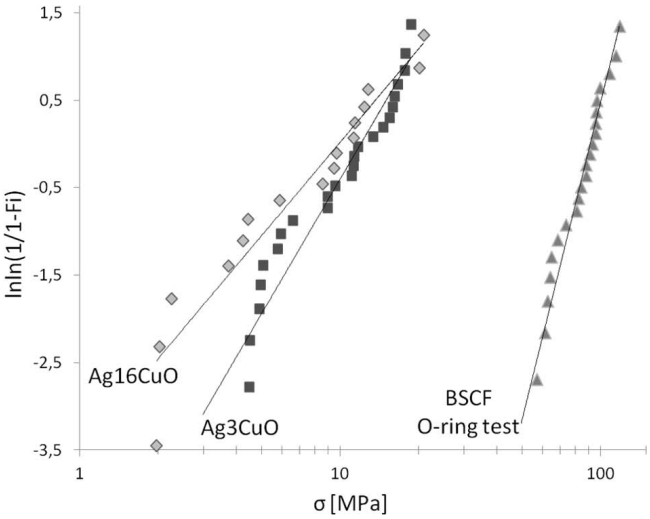

Fig. 12: Weibull diagram of the tensile tests for bond specimens with Ag3CuO and Ag16CuO braze along with results of an O-ring test for monolithic BSCF tubes (outer diameter = 15.5 mm, length = 10 mm, wall thickness = 0.85 mm).

The Weibull diagram represents the scatters in tensile strength of both braze joint options. The Weibull modulus m can be regarded as a measure of the scatter in strength and thus of the reproducibility of the brazing process. According to Eq. (3), the strength of ceramic components depends on the volume of the component and the effective volume depends on the Weibull modulus m. Thus lower m values result in a higher scatter of strength in the case of a high effective volume. Effective volume in the tensile test is approx. 35 times higher (391 mm³) than in the O-ring test (11 mm³). Further, the Weibull plots show that the tensile strength level is relatively low for both brazes Ag3CuO and Ag16CuO compared to the strength of monolithic BSCF tubes determined in the O-ring test. Metallurgical reactions in the joint materials, the growth of the reaction zones as well as formation of big pores in the BSCF alter the base materials and can be considered as factors influencing the level and scatter of the joint strength. Furthermore it cannot be ruled out that superimposed bending owing to misalignment of the joint itself or the imperfect assembly of the specimen in the test rig reduces the strength level. The Weibull parameters for both braze options and the monolithic BSCF are summarized in Table 5.

As mentioned earlier, the primary failure mode of the brazed joints is observed in the ceramic close to the joint interface. FEA predicts the location of the maximum stress after cooling from 955 °C to 20 °C on the inner BSCF tube surface close to the interface. The residual stress state in a section of the BSCF ceramic is illustrated with the distribution of first principal stress in Fig. 13 (b). The maximum principal stress in the BSCF after cooling to room temperature is found to be 37 MPa and has an axial direction vector. These axial tensile stresses may superimpose with the applied tensile force during testing and further reduce joint strength. The maximum principal stress distribution in the BSCF ceramic after cooling to room temperature and a superimposed tensile force of approx. 570 N are shown in Fig. 13 (c), where the magnitude is found to be 54 MPa and again has an axial direction vector.

For every specimen tested the crack appears in the ceramic, close to the brazing layer. One reason can be found with the numerical simulation described above. The simulations show that the highest normal stresses appear in the ceramic close to the brazing layer (see Fig. 13). This fact might explain the location of crack initiation but not the differences in strength between the two brazing compositions. The stresses depend on differences in thermal expansion and elastic constants. With an increase in the CuO content in the braze alloy, it can be expected that the coefficient of thermal expansion will decrease by only a minimal extent to a value closer to the thermal expansion coefficient of the BSCF and steel. This slight influence cannot be the explanation for the differences in tensile strength. Consequently, it can be expected that the major reason for the difference in tensile strength in case of the Ag3CuO- and the Ag16CuO-bonded specimens depends on the different magnitudes of the affected zones in the microstructure of the BSCF, as explained in Section 3.1.

Table 5: Weibull parameters of the tensile tests.

Specimen	Characteristic strength σ_0 [MPa]	Weibull modulus m	Effective volume [mm³]
BSCF-Ag3CuO-AISI 314- joint	14	2.2	391
BSCF-Ag16CuO-AISI 314- joint	11	1.5	391
Monolithic BSCF tube	95	5.3	11

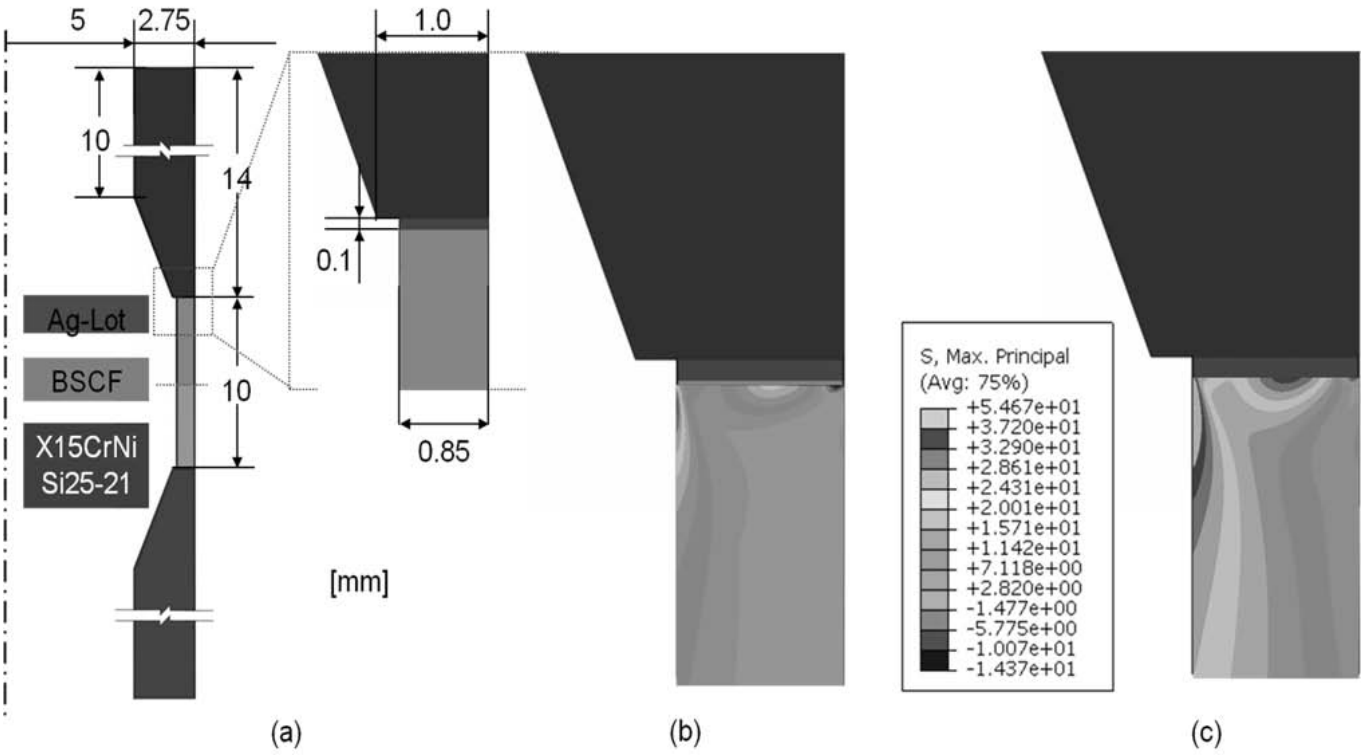

Fig. 13: Joint geometry (a) and distribution of the maximum principal stress (in MPa) in a section of the BSCF ceramic after cooling from brazing temperature at 955 °C to room temperature (b) and superimposed tensile load (c).

IV. Conclusion

Wetting tests show that with reactive air brazing of BSCF with AgCuO braze the contact angle on the ceramic decreases with increasing CuO content in the braze. In this work, braze alloys with CuO concentrations of 1 mol% up to 16 mol% were used. A high CuO content in the braze results in better wettability. But a change in the microstructure of the ceramic was also observed. The reason is chemical corrosion owing to CuO diffusion at the grain boundaries of the BSCF and a chemical bond of copper-cobalt mixed oxides, accompanied with local re-sintering of the BSCF during the brazing process. The resulting microstructure in the affected zone is characterized by higher porosity with larger and irregularly distributed pores and enlarged grains with copper-cobalt-oxide phases at the grain boundaries.

Mechanical tensile tests on ceramic/steel joints with Ag3CuO braze and Ag16CuO braze show that the specimens with the high CuO content in the braze alloy exhibit lower mechanical strength. Based on the fact that all specimens cracked in the ceramic close to the brazing seam, it can be expected that the cracks started at defects in the affected layer of the ceramic. The wetting tests show that the affected layer in the case of the specimens with the Ag16CuO braze is much thicker and more pronounced than in the case of the specimens with the Ag3CuO braze. That appears to be the reason for the differences in the mechanical strength. The characteristic fracture strength σ_0 of the BSCF/AISI 314 brazed tensile specimens, tested at ambient temperature is 14 MPa for the Ag3CuO braze and 11 MPa for the Ag16CuO braze.

Acknowledgements

The authors gratefully acknowledge financial support by DFG under contract No. PAK 524.

References

1 Ovenstone, J., Jung, J., White, J.S., Edwards, D.D., Misture, S.T.: Phase stability of BSCF in low oxygen partial pressures, *J. Solid State Chem.*, **181**, 576 – 586, (2008).

2 Kneer, R., Toporov, D., Förster, M., Christ, D., Broeckmann, C., Pfaff, E.M., Zwick, M., Engels, S., Modigell, M.: OXY-COAL-AC: Towards an integrated coal-fired power plant process with ion transport membrane based oxygen supply, *Energ. Environ. Sci.*, 198 – 207, (2010).

3 Dabbarh, S., Pfaff, E.M., Ziombra, A., Bezold, A.: Brazing of MIEC ceramics to high temperature metals, ceramic transactions, Wiley-VCH, 213 – 223, (2010).

4 Wang, H., Cong, Y., Yang, W.: Oxygen permeation study in a tubular $Ba_{0.5}Sr_{0.5}Co_{0.8}Fe_{0.2}O_{3-\delta}$ oxygen permeable membrane, *J. Membrane Sci.*, 210, 259 – 271, (2002).

5 Shao, Z., Yang, W., Cong, Y., Dong, H., Tong, J., Xiong, G.: Investigation of the permeation behavior of a BSCF oxygen membrane, *J. Membrane Sci.*, **172**, 177 – 188, (2000).

6 US-Patent No. US 7,055,733 B2, Weil *et al.*: Oxidation ceramic to metal braze seals for applications in high temperature electrochemical devices and method of making, (2006).

7 Kim, J.Y., Hardy, J.S., Weil, K.S.: Effects of CuO content on the wetting behavior and mechanical properties of a Ag-CuO braze for ceramic joining, *J. Am. Ceram. Soc.*, **88**, 2521 – 2527, (2005).

8 Weil, K.S., Hardy, J.S., Rice, J.P., Kim, J.Y.: Brazing as a means of sealing ceramic membranes for use in advanced coal gasification process, *Fuel*, **85**, 156 – 162, (2006).

9 Weil, K.S., Coyle, C.A., Darsell, J.T., Xia, G.G., Hardy, J.S.: Effects of thermal cycling and thermal aging on the hermeticity

and strength of silver-copper oxide air-brazed seals, *J. Power Sources*, **152**, 437 – 447, (2005).

10 Schüler, C.C., Stuck, A., Beck, N., Keser, H., Täck, U.: Direct silver bonding – an alternative for substrates in power semiconductor packaging, *J. Mater. Sci.: Mater. El.*, **11**, 389 – 396, (2000).

11 Hardy, J.S., Kim, J.Y., Weil, K.S.: Joining mixed conducting oxides using an air-fired electrically conductive braze, *J. Electrochem. Soc.*, **151,** [8], J43 – J49, (2004).

12 Weil, K.S., Hardy, J.S., Kim, J.Y.: Development of brazing technology for use in high-temperature gas separation equipment, 17th annual conference on fossil energy materials, Baltimore, MD (US), 04/22/2003 – 04/24/2003

13 Weil, K.S., Hardy, J.S.: Development of a new ceramic-to-metal brazing technique for oxygen separation/generation applications, 16th annual conference on fossil energy materials, (2002).

14 Bobzin, K., Schläfer, T., Kopp, N.: Thermochemistry of brazing ceramics and metals in air, *Int. J. Mater. Res.,* **102**, 972 – 976, (2011).

15 Kaletsch, A., Pfaff, E.M., Broeckmann, C., Nauels, N., Modigell, M.: Pilot module for oxygen separation with BSCF membranes, dechema (Eds.): Book of extended abstracts: Efficient carbon capture for coal power plants, 137 – 143, (2011).

16 Pfaff, E.M., Kaletsch, A., Broeckmann, C.: Design for a MIEC oxygen transport membrane pilot module, *Chem. Eng. Technol.*, article in press

17 Stephens, J.J., *et al.*: Update on creep of silver alloy, Internal memo to M.K. Neilsen, Sandia national laboratories, (1996)

18 Malzbender, J., Huang, B., Moench, B., Steinbrecht, R.W.: A comparison of results obtained using different methods to assess the elastic properties of ceramic materials exemplified for $Ba_{0.5}Sr_{0.5}Co_{0.8}Fe_{0.2}O_{3-\delta}$, *J.Mater. Sci.*, **45**, 1227 – 1230, (2010).

19 Kim, J.Y., Hardy, J.S., Weil, K.S.: Silver-copper oxide based reactive air braze for joining yttria-stabilized zirconia, *J. Mater. Res.*, **20**, [3], (2005).

20 Driessens, F.C.M., Rieck, G.D., Coenen, H.N.: Phase equilibria in the system cobalt oxide/Copper Oxide in Air, *J. Inorg. Nucl. Chem.*, 30, 747 – 753, (1968).

21 Zabdyr, L.A., Fabrichnaya, O.B.: Phase equilibria in the cobalt oxide – copper oxide system, *J.Phase Equilib.*, **23**, [2], (2002).